

Laser-intensity dependence of the multielectron ionization of CO at 305 and 610 nm

J. Lavancier, D. Normand, C. Cornaggia, J. Morellec, and H. X. Liu

Service de Physique des Atomes et des Surfaces, Centre d'Etudes Nucléaires de Saclay, 91191 Gif-sur-Yvette CEDEX, France

(Received 18 July 1990)

We have studied the multielectron dissociative ionization of CO in the range of 10^{13} – 10^{15} W/cm² (laser wavelength 305 and 610 nm; pulse duration 1.4 and 2 ps, respectively). By measuring the fragment kinetic energies and laser-intensity dependences, we have investigated the detailed dynamics of the interaction process. At 610 nm, the formation of CO³⁺ and CO⁴⁺ occurs as the molecule dissociates. The transitions occur at well-defined internuclear distances that are shown to be independent of the peak laser intensity. At 305 nm, the ionization processes are found to progress in a different way: CO is multiphoton multiply ionized at the equilibrium internuclear distance of the molecule. This vertical excitation yields fragments with charge states and initial energies lower than at 610 nm. The comparison with the previous results obtained on N₂ is discussed.

I. INTRODUCTION

The interaction of diatomic molecules with intense sub-picosecond or picosecond laser pulses (peak power 10^{15} – 10^{16} W/cm²) has been actively studied over the past few years. The experiments have been carried out on several gaseous species such as H₂ (Refs. 1,2), N₂ (Refs. 3–5), CO (Ref. 6), and HI (Ref. 7). Except for H₂, the interaction leads to the formation of transient multicharged molecular ions that dissociate into energetic ionic fragments.

Two mechanisms have been invoked to account for the experimental results. The interaction of 248-nm laser radiation with N₂ molecules produces atomic fragments whose initial kinetic energies are consistent with the ionization of the parent ions at the equilibrium internuclear distance of N₂.^{3,8} Moreover, it appears that the charge asymmetric dissociation channels are favored at this wavelength (e.g., N₂⁴⁺ → N³⁺ + N⁺). The rapid energy transfer leading to vertical molecular transitions and the tendency to produce charge asymmetric dissociation are assumed to be the consequence of a large dipole moment arising from a multielectron motion along the laser polarization. At 305 nm, our results are also in agreement with this interpretation.⁵ Around 600 nm, the dissociation processes of N₂ show a different tendency.^{4,5} First, the charge asymmetric reactions are not favored at this wavelength. On the contrary, the formation of the N²⁺ + N²⁺ ion pair is found to be the dominating dissociative path. Second, the ionization processes appear to be nonvertical: the electrons are sequentially stripped away during the molecular dissociation at given internuclear separations. This unexpected phenomenon is discussed by Codling *et al.* in terms of a simple field ionization model.⁹ Moreover, the molecular structure is also expected to play a preponderant role up to the formation of N₂⁴⁺ ions for which the molecular coupling can then be described by the Coulombic interaction between the two atomic constituents.⁵

In order to have a better understanding about the role

of the molecular structure on the interaction process molecule radiation, we have studied the CO molecule when irradiated by an intense picosecond laser radiation. In our experiment, the ionization and fragmentation mechanisms are deduced from the energy measurements of the dissociation products and from the ion yield dependence on the laser intensity in the range of 10^{13} – 10^{15} W/cm². To investigate the role of the laser wavelength, the experiment is repeated at 610 and 305 nm. The paper is organized as follows. The results are presented in Sec. III (610 nm) and Sec. IV (305 nm) after the description of the experimental setup given in Sec. II. The conclusion is given in Sec. V.

II. EXPERIMENTAL SETUP

The experimental arrangement, including the laser system, has already been described in detail elsewhere.⁵ Briefly, the basic components of the experimental setup are the following. The pulses delivered by a synchronously pumped dye laser are amplified through a four-stage dye amplifier pumped by a Nd-YAG laser (where YAG denotes yttrium aluminum garnet) operating at 10 Hz. The measurements of the laser-pulse characteristics give a pulse energy of a few mJ and a pulse duration of 2 ps at 610 nm. The 305-nm laser radiation is obtained after frequency doubling in a BBO crystal (conversion efficiency 15%) which shortens the laser-pulse duration to 1.4 ps at this wavelength. The laser light is focused by a spheroparabolic lens of 60-mm focal length for the 305-nm experiment; alternatively a lens of 150-mm focal length is used for the 610-nm experiment that permits one to obtain comparable laser intensities at both wavelengths and to avoid saturation effects. The focal sections are determined by photometric measurements¹⁰ and are found to be 7.8×10^{-7} cm² at 305 nm and 1.3×10^{-6} cm² at 610 nm leading to maximum peak powers of 3×10^{14} W/cm² at 305 nm and 10^{15} W/cm² at 610 nm.

The detection system consists of a double chamber time-of-flight (TOF) ion mass spectrometer pumped at a

background pressure of 10^{-9} Torr.¹¹ The application of a weak collection electric field in the interaction chamber makes possible the determination of the fragment kinetic energies with a good precision (10%) whereas the second chamber strongly accelerates the ions to ensure a good collection efficiency. Finally, the ions are mass separated through an 18-cm-long drift tube and give a signal which feeds a Lecroy model 9400 Transient Digitizer with a 100-MHz sampling frequency.

III. STUDY AT 610 nm

A. Experimental results

The application of a strong extraction field in the interaction region gathers the ions of a given charge and mass into a single peak regardless of their initial kinetic energies. Under these conditions we obtain the TOF ion mass spectrum of CO represented in Fig. 1 recorded at a laser intensity of 10^{15} W/cm². The interaction produces two charge states of oxygen fragments (O^+ and O^{2+}) and three charge states of carbon ions (C^+ , C^{2+} , and C^{3+}), the CO^+ signal being always predominant in the intensity range investigated. We note that the O^+ and C^+ ion abundances are almost equal whereas the C^{2+} ion peak is about four times larger than the O^{2+} peak. In the same intensity range these ionic species have also been observed by Codling *et al.*⁶ but surprisingly, the dissociation rates are much stronger in the present experiment. This is presumably an effect of the laser-pulse duration which is three times longer in our experiment. Due to the very low operating pressure (4×10^{-8} Torr), we also observe the contributions of some spurious species such as H^+ and H_2O^+ . Interestingly, no peak arising from metastable CO^{2+} is observed at this wavelength whereas doubly charged molecules are an important feature in the TOF spectra of N_2 (Ref. 5) and especially O_2 .¹²

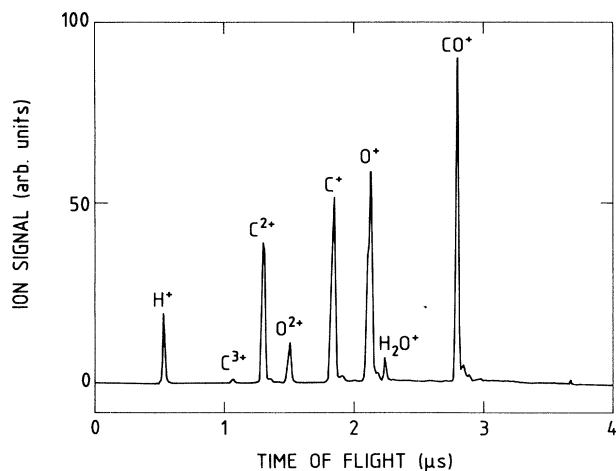


FIG. 1. TOF ion mass spectrum of CO produced with intense picosecond 610-nm irradiation (peak intensity 10^{15} W/cm²). The extraction field in the interaction chamber is 700 V/cm and the CO pressure is 4×10^{-8} Torr.

The initial kinetic energies of the fragments are then measured by decreasing the collection electric field in the interaction chamber. When this latter is adjusted at 50 V/cm and when the laser E field lies along the axis of detection, we get the typical TOF ion mass spectra represented in Figs. 2(a) and 2(b) corresponding to two different laser intensities. We note that the signal of each ion species is characterized by two symmetric components. One arises from fragments that are initially ejected towards the detector. The other one is related to fragments initially directed away from the detector and whose momenta have been reversed by the extraction field. The initial kinetic energies of the fragments are then simply deduced from the time interval separating two associated peaks and from the extraction field value in the interaction chamber. It must be noted that following dissociation, the total kinetic-energy release is distributed between the two fragments, C^{q+} and O^{p+} , in inverse ratio to their masses according to the relation

$$m(C^{q+})E(C^{q+}) = m(O^{p+})E(O^{p+}). \quad (1)$$

However, the energy measurements can be perturbed by the space-charge effects so that we have performed a study to evaluate the influence of the CO pressure in the interaction cell. Figure 3 represents the energy variation

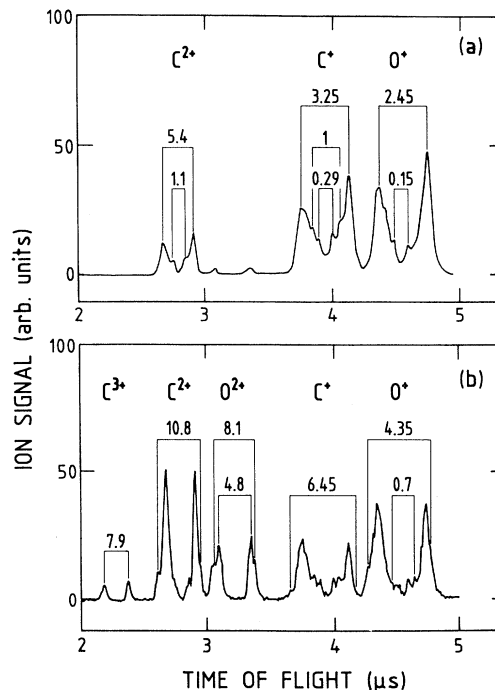


FIG. 2. TOF ion mass spectra of CO recorded at 610 nm at two increasing laser intensities: (a) 6×10^{13} W/cm², (b) 10^{15} W/cm². In each case the extraction field is set to 50 V/cm so as to distinguish the different classes of velocities for each group of atomic ions. The arrows point at the backward and forward ion pairs whose initial kinetic energies (expressed in eV) are indicated above. The CO pressure is adjusted to achieve a constant ion yield.

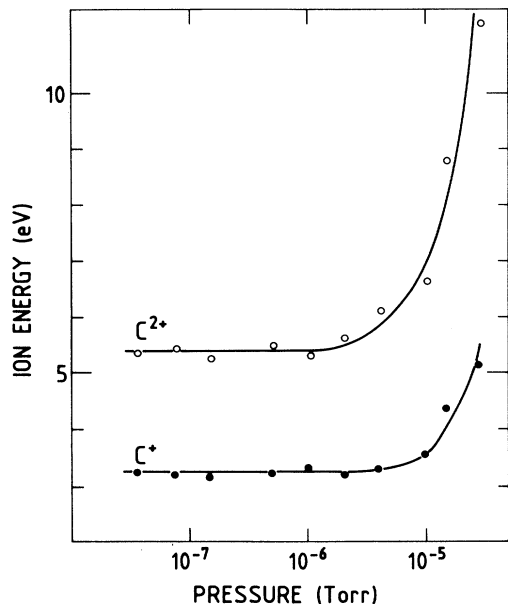


FIG. 3. Initial kinetic energies of one velocity class of C^+ and C^{2+} ions measured as a function of the operating pressure in the interaction chamber. At 10^{15} W/cm² the space-charge effects appear when the CO pressure goes beyond 2×10^{-6} Torr and result in an increase of the ion initial energies.

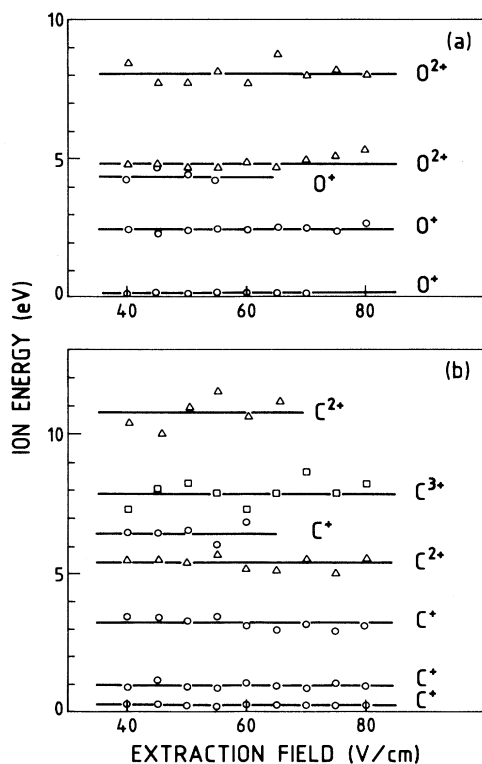


FIG. 4. Initial kinetic energies of (a) O^{p+} fragments and (b) C^{q+} fragments, respectively, measured as a function of the extraction electric field. The average values of the ion energies are represented by horizontal lines. The energy relative uncertainty is estimated to be 10%.

of one energy class of C^+ and C^{2+} ions as a function of the operating pressure at 10^{15} W/cm². From 2×10^{-6} Torr, the initial kinetic-energy determinations are distorted by the space charge in that it increases the ion energies (as well as the widths of the peaks). Therefore we have carried out the experiment with operating pressures below 10^{-6} Torr in order to avoid any space-charge effects.

As shown in Figs. 4(a) and 4(b), the energy measurements are performed for various extraction fields ranging from 40 to 80 V/cm. This method makes it possible to improve the determinations of the ion energies whose average values are indicated by horizontal lines. We note that the energies of several ionic species can only be determined with low extraction fields. Given the statistical errors and the digitizer electronic width, the relative uncertainty in the ion energy measurements is evaluated to be about $\pm 10\%$.

Finally, we have also studied the variation of the ion signals as a function of the laser intensity and plotted the results in log-log coordinates in Fig. 5. This study is intended to confirm a possible correlation between a C^{q+} fragment and an O^{p+} one arising from the same $CO^{(p+q)+}$ parent ion and thus presenting the same depen-

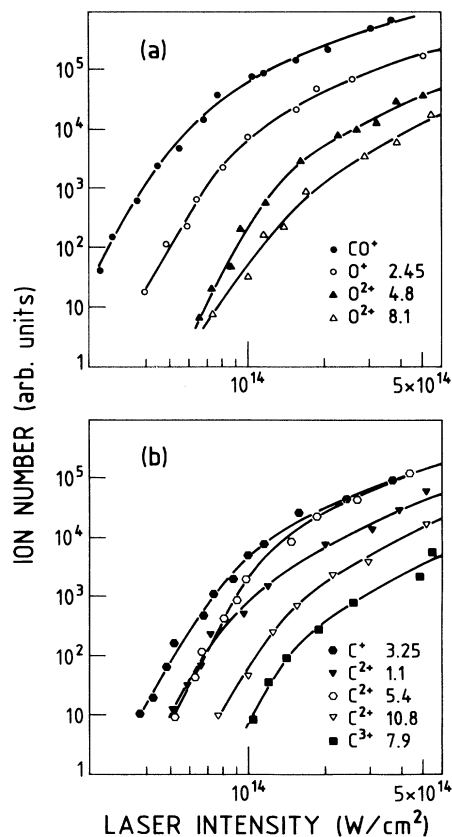


FIG. 5. Number of atomic ions detected as a function of peak laser intensity at 610 nm: (a) O^{p+} fragments, (b) C^{q+} fragments. The different classes of ion fragments are identified by their respective energies indicated in eV.

TABLE I. Initial kinetic energies and power laws of the different ion classes at 610 nm. The abundances of several ionic species are too weak to allow the determination of the k values.

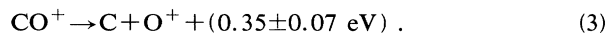
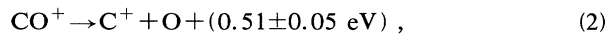
	Initial energy (eV)	Power law (K)
CO ⁺	0	7.5±0.6
O ⁺	0.15±0.03	5.5±0.6
	0.70±0.10	
	2.45±0.25	7.5±0.4
	4.35±0.50	
C ⁺	0.29±0.03	
	1.00±0.15	
	3.25±0.35	7.6±0.6
	6.45±0.70	
O ²⁺	4.8±0.5	8.7±0.8
	8.1±0.8	6.3±1.0
C ²⁺	1.10±0.15	7.1±0.7
	5.4±0.6	8.3±0.8
C ³⁺	10.8±1.1	7.2±0.8
	7.9±0.9	8.3±0.9

dence on the laser intensity. We note that each ion curve presents a saturation part which is a typical effect of multiphoton experiments due to the depletion of the initial state of the corresponding ion. Below saturation, the power dependence of a given ion class is characterized by the power law k , obtained by measuring the slope of the ion curve. The power laws and the kinetic-energy values of the different ion species are summarized in Table I.

B. Discussion

When the laser intensity is reduced down to 3×10^{13} W/cm², we essentially detect molecular CO⁺ ions. The 14-eV ionization energy of CO is then reached by the absorption of at least seven photons at 610 nm ($h\nu = 2.03$ eV).

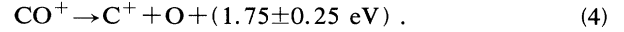
As shown in Fig. 2(a), several species of atomic ions appear at higher intensity (6×10^{13} W/cm²). In particular we detect two classes of slow ions corresponding to 0.29-eV C⁺ and 0.15-eV O⁺ fragments. The energies of these ions do not fulfill relation (1) so that they cannot arise from the same parent ion CO²⁺. In addition, the dissociation of a CO²⁺ molecule would lead to the formation of faster ions. These C⁺ and O⁺ ions cannot proceed either from the dissociation or predissociation of the neutral molecule followed by the multiphoton ionization (MPI) of the fragments. Indeed, the preponderance of the CO⁺ signal at low intensity implies that the molecule ionization precedes the molecular fragmentation. Consequently, the 0.29-eV C⁺ and 0.15-eV O⁺ result from two different channels involving the dissociation of CO⁺ according to



These two dissociative mechanisms occur after the extinction of the laser pulse since we do not observe any

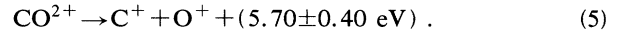
subsequent ionization of the fragments.

Similarly, the 1.00-eV C⁺ ions are produced from CO⁺ molecules via a third dissociation channel:



On the other hand, we detect a slow C²⁺ ion class whose measured energy (1.1 eV) is too small to account for a process involving the dissociation of a multicharged molecule. These ions are more likely generated by atomic MPI of the C⁺ ions created by reaction (4). This implies that reaction (4) occurs in less than 2 ps (the laser-pulse duration). We would also expect to observe the MPI of the neutral O fragments associated with the C⁺ ions; these ions would have an initial kinetic energy of 0.75 eV. However, the abundance of these ions is too weak at 6×10^{13} W/cm² so that they only appear as shoulders in the main peak of O⁺ ions. They are more easily detected at higher intensity [see Fig. 2(b)].

The two major contributions of Fig. 2(a) correspond to 3.25-eV C⁺ and 2.45-eV O⁺ ions whose energies fulfill relation (1). In addition, we verify in Fig. 5 that the two ion signals have the same abundances and the same dependences on the laser intensity. Thus the 3.25-eV C⁺ and 2.45-eV O⁺ fragments are interpreted as resulting from the dissociation of CO²⁺ molecular ions according to the reaction

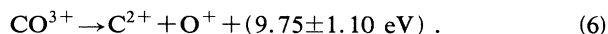


Several quasibound (or unbound) states of CO²⁺ can account for ions with such initial kinetic energies (see the *ab initio* calculations of Wetmore *et al.*,¹³ Larsson *et al.*,¹⁴ and Lablanquie *et al.*¹⁵). By comparing the kinetic energy released in reaction (5) with those obtained by electron impact^{16–18} and synchrotron radiation,¹⁹ the involved CO²⁺ states are assumed to be the low-lying $1^1\Sigma^+$, $1^1\Pi$, and $1^3\Pi$ states. Interestingly, the non-resonant laser excitation creates CO²⁺ states with a higher selectivity than the other methods of excitation that populate a large number of molecular states.

The agreement with the synchrotron radiation data indicates that the multiphoton transitions occur at the equilibrium internuclear distance of CO (1.13 Å). Indeed, due to the prominence of the CO⁺ signal, the production of CO²⁺ ions must proceed from a sequential ionization involving low-lying intermediate states of CO⁺ for which the change in the internuclear separation is small. For example, the CO²⁺ ions can be populated by a sequential mechanism involving a 14-photon absorption process from the ground state of CO⁺. Finally, it is worth noting that all the molecular states of CO²⁺ populated during the interaction process have led to the dissociation of the molecule (with a lifetime inferior to a few μs) since no peak arising from metastable CO²⁺ has been detected.

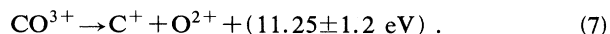
At 6×10^{13} W/cm², we also detect C²⁺ ions with 5.4-eV kinetic energies that are assumed to proceed from the dissociation of CO³⁺. In our opinion the associated O⁺ ion signal is too weak to be resolved at this intensity level due to the presence of the strong 2.45-eV O⁺ ion population. On the contrary, when the laser intensity is increased [Fig. 2(b)], we detect 4.35-eV O⁺ fragments

which have the correct energy to be correlated to the 5.4-eV C^{2+} ions (the signals of the two ionic species differ by a factor of 2 due to the response of the electron multiplier CuBeO cathode²⁰). Indeed, at 10^{15} W/cm², the CO^{2+} ions tend to be ionized into CO^{3+} rather than being dissociated which cuts down reaction (5) and favors the following dissociation process:



Considering that the molecular coupling of CO^{3+} can be described by the Coulombic repulsion between the two fragments, then the triple ionization of CO at its equilibrium internuclear distance would produce fragments with much greater initial energies (about 14 eV for C^{2+}). We must then consider that CO^{3+} is created at a larger internuclear distance. Indeed, as observed previously on N_2 (Refs. 4,5) and HI (Ref. 7) at 600 nm, the ejection of the third electron occurs as the double charged molecular ion dissociate. Taking into account the total energy supplied to the fragments in reaction (6), the CO^{3+} ions are created at the internuclear separation $r = 2.95 \text{ \AA}$ (Fig. 6).

An important contribution of O^{2+} ions is also detected at 10^{15} W/cm². In particular, 4.8-eV O^{2+} ions have appeared along with fast 6.45-eV C^+ ions. The energies of these ions fulfill perfectly relation (1) so that they are certainly generated by the reaction



This dissociation channel occurs at higher laser intensity than reaction (6) which is consistent with the energy gaps between the Coulombic repulsion curves represented in Fig. 6. However, the triple ionization of CO occurs at smaller internuclear distance in reaction (7), i.e., $r = 2.55 \text{ \AA}$. Our observation implies that as the laser pulse develops, the "newly" formed CO^{2+} ions can be ionized according to two competing channels converging into the $C^+ + O^{2+}$ or the $C^{2+} + O^+$ ion pairs, the latter being always predominant. It must be noted that the 4.8-eV O^{2+} signal is too large to be entirely correlated to the 6.45-eV C^+ one. Indeed, part of the 4.8-eV O^{2+} detected ions

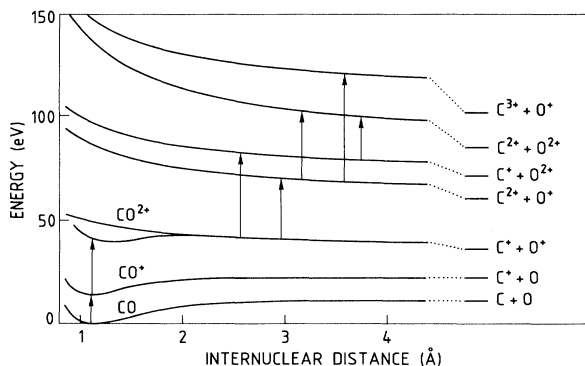
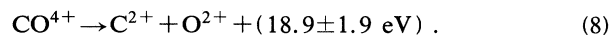


FIG. 6. Simplified potential-energy diagram of CO showing the ionization and dissociation events occurring at 610 nm. From CO^{3+} the molecular coupling is described by the Coulombic repulsion between the two atomic fragments.

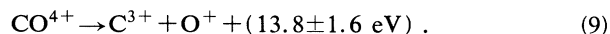
might be associated with some C^{2+} ions whose contribution is too weak to be observed in the shoulders of the big 5.4-eV C^{2+} peak. This association would imply the occurrence of the reaction $CO^{4+} \rightarrow C^{2+} + O^{2+} + 11 \text{ eV}$ observed in another experiment.⁶

As can be seen in Fig. 2(b), fast atomic dications are observed corresponding to 10.8-eV C^{2+} and 8.1-eV O^{2+} fragments. The energies of these ions fulfill relation (1). Moreover, Fig. 5 shows that the two signals present the same amplitudes and an identical dependence on the laser intensity. Therefore we assume that the 10.8-eV C^{2+} and 8.1-eV O^{2+} fragments proceed from the fragmentation of the same parent ion according to



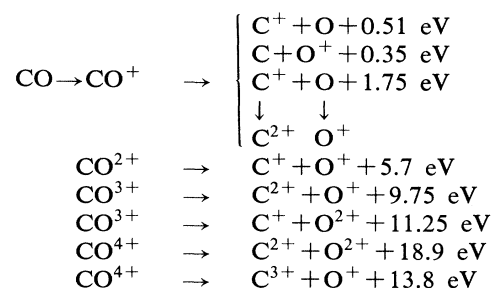
The fourth ionization of CO can occur as CO^{3+} dissociate into $C^{2+} + O^+$ (at $r = 3.15 \text{ \AA}$) and/or $C^+ + O^{2+}$ (at $r = 3.75 \text{ \AA}$) ion pairs.

Finally we note that a weak contribution of C^{3+} ions with 7.9-eV kinetic energy is detected. They are likely to be associated with O^+ ions whose observation is difficult due to their weak abundance (considering the detector response, the O^+ signal is expected to be about three times smaller than the C^{3+} signal). Consequently, the C^{3+} ions are supposed to result from the dissociation of CO^{4+} molecules according to



The CO^{4+} ions involved in reaction (9) are found to be formed from CO^{3+} dissociating to the $C^{2+} + O^+$ separated atom limit at the internuclear distance of 3.6 Å (Fig. 6).

The processes occurring at 610 nm can be summarized in the following diagram:



The processes suggested above are in agreement with those observed by a covariance mapping technique (using a laser of 600 nm, pulse length 0.6 ps, and focused intensity 3×10^{15} W/cm²) (Ref. 6) although the measured energies are slightly different in some channels. In both experiments, the results show that the CO molecule is sequentially ionized as the molecule dissociates. Moreover, considering that the fragments are created with well-defined initial kinetic energies, we must admit that the successive ionization steps occur at given internuclear separations. Surprisingly, the initial energies of the fragments are found to be independent of the peak laser intensity. The transitions occurring around $r = 3 \text{ \AA}$, the chemical forces may still be involved in the molecular coupling in competition with the Coulomb repulsion be-

tween the two fragments. This could lead to the occurrence of laser-induced quasiresonances for given r values which would strongly enhance the ionization probabilities. In this interpretation, the molecular dissociating ion "chooses" the intensity adequate to establish the conditions of dynamic resonances: when the peak laser intensity is increased, the resonance intensity is found in outer parts of the interaction volume where the ionization event takes place. Analogous processes have been invoked to interpret the photoelectron spectra on rare gas atoms in the same intensity range.^{21,22}

IV. STUDY AT 305 nm

A. Experimental results

The interaction of CO molecules with 305-nm laser radiation (peak intensity 3×10^{14} W/cm²) leads to the TOF ion mass spectrum represented in Fig. 7. We confirm the tendencies observed previously in the N₂ studies,⁵ i.e., (i) the maximum charge state of the fragments detected at 305 nm is lower than at 610 nm at the same intensity. Two major peaks of single charged ions are observed (C⁺ and O⁺) along with a smaller peak of C²⁺ and a minor contribution of O²⁺ ions. (ii) The dissociation rate is strongly increased at 305 nm. We note that a very small peak can be associated to the detection of metastable CO²⁺ ions with lifetimes in the μ s range.

Figures 8(a)–8(c) show TOF spectra of the ionic fragments recorded at three increasing laser intensities with an extraction field of 50 V/cm. The ions with the higher charge states and/or higher velocities appear as the laser intensity is increased. As at 610 nm, the initial kinetic energies of the fragments are determined by recording several spectra associated with different extraction fields [Figs. 9(a) and 9(b)]. It must be noted that at 305 nm and 3×10^{14} W/cm², the space-charge effects only appear for operating pressures as high as 3×10^{-5} Torr.

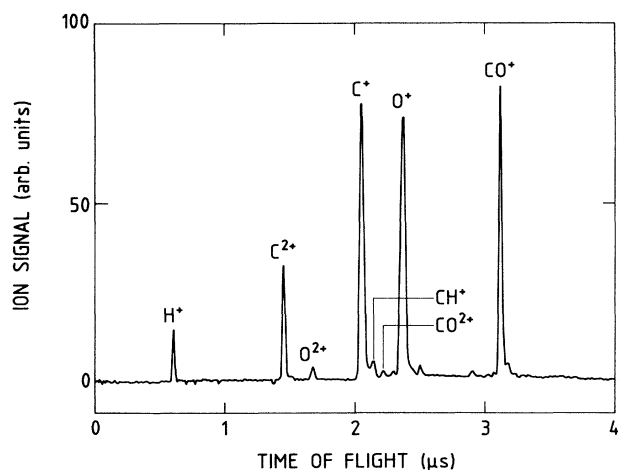


FIG. 7. TOF ion mass spectrum of CO observed at 3×10^{14} W/cm² using a 305 nm, 1.4-ps laser radiation. The pressure in the interaction region is 5×10^{-7} Torr and the extraction field is 700 V/cm.

Finally we have also measured the ion abundances as a function of the laser intensity in the range of 4×10^{13} to 3×10^{14} W/cm². For the sake of clarity, the results for the carbon and oxygen ions are presented in Figs. 10(a) and 10(b), respectively. The experimental results (power laws and initial kinetic energies of the ions) are summarized in Table II.

B. Discussion

For laser intensities below 4×10^{13} W/cm², no fragmentation product is detected (Fig. 10). We only observe CO⁺ ions created with a power law of about 4, in agreement with the nonresonant ionization of CO molecules by at least four photons at 305 nm ($h\nu = 4.06$ eV).

When the laser intensity is increased up to 8×10^{13} W/cm², singly charged fragments appear on the TOF spectrum of CO [Fig. 8(a)]. The C⁺ signal is characterized by a main peak which is not divided into its two components and thus corresponds to ions with near zero initial kinetic energies (< 0.1 eV). We also detect slow O⁺ ions whose initial energies are found to be 0.53 eV. Given the low energies of these two ionic species (Table

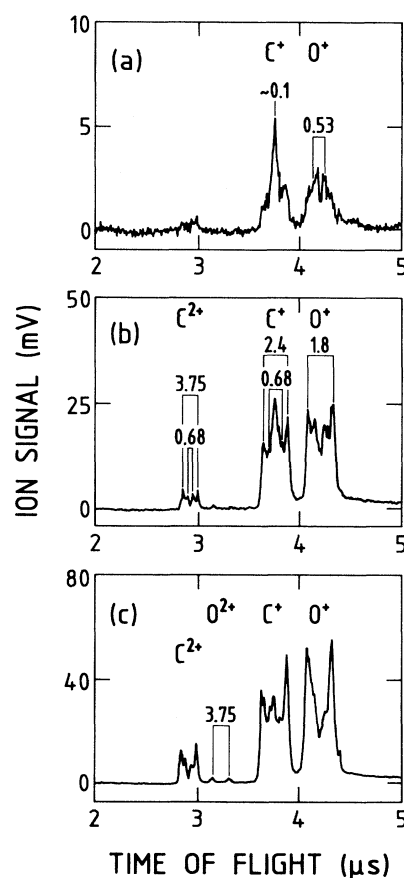


FIG. 8. TOF ion mass spectra of CO recorded at 305 nm at three increasing laser intensities: (a) 8×10^{13} W/cm²; 8×10^{-6} Torr; (b) 10^{14} W/cm²; 8×10^{-6} Torr; (c) 3×10^{14} W/cm²; 8×10^{-7} Torr. The extraction field is 50 V/cm.

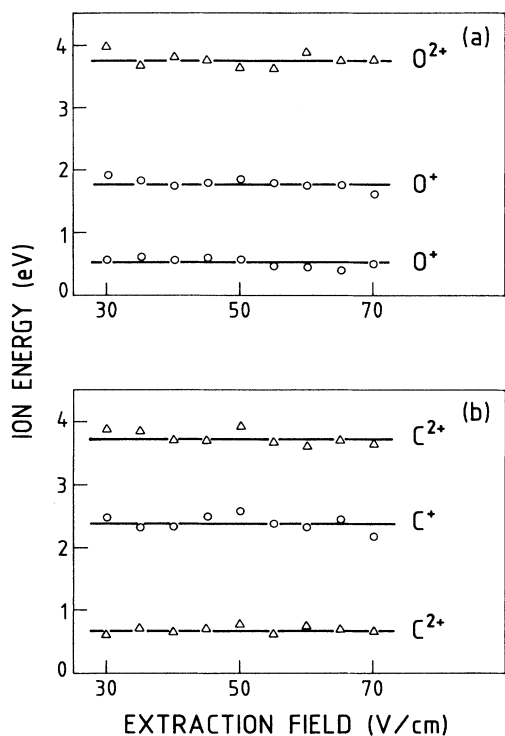
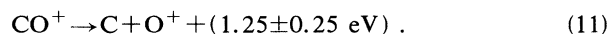


FIG. 9. Initial kinetic energies of (a) O^{p+} fragments and (b) C^{q+} fragments, respectively, measured as a function of the extraction field. The lines indicate the average values of the measurements (the energy relative uncertainty is about 10%).

II), they are assumed to arise from the dissociation of CO^+ according to the reactions

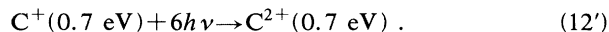
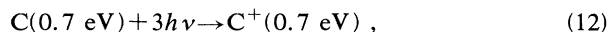


The peak shoulders are associated with small contributions of faster ions whose energies cannot be determined with accuracy at this laser intensity.

TABLE II. Initial kinetic energies and power laws of the different ion classes at 305 nm. The observation of the 0.68-eV C^+ ions is too difficult to allow an accurate determination of the k value.

	Initial energy (eV)	Power law (K)
CO^+	0	3.9 ± 0.3
O^+	0.53 ± 0.10	5.0 ± 0.2
	1.8 ± 0.2	6.5 ± 0.3
C^+	< 0.1	5.2 ± 0.3
	0.7	
	2.40 ± 0.25	6.5 ± 0.7
O^{2+}	3.75 ± 0.40	6.9 ± 0.9
C^{2+}	0.68 ± 0.07	6.3 ± 0.7
	3.75 ± 0.40	9.8 ± 1.1

At 10^{14} W/cm^2 [Fig. 8(b)], we detect two charge states of carbon ions (C^+ and C^{2+}) whose energies are equal to those of the neutral fragments undetected in reaction (11). This reaction is then assumed to occur before the extinction of the laser pulse, the atomic fragments being subsequently ionized during the remainder of the pulse:



We do not observe any multiphoton ionization of the O^+ fragment which is certainly related to the high ionization level of this species (35.1 eV instead of 24.4 eV for C^+). Concerning reaction (10), we do not observe the subsequent ionization of the C^+ and O fragments which implies that the lifetime of the involved CO level is longer than the laser-pulse duration.

As shown in Fig. 8(b), faster C^+ (2.4 eV) and O^+ (1.8 eV) fragments become easily detectable at 10^{14} W/cm^2 . We note that the energies of these two classes of ions

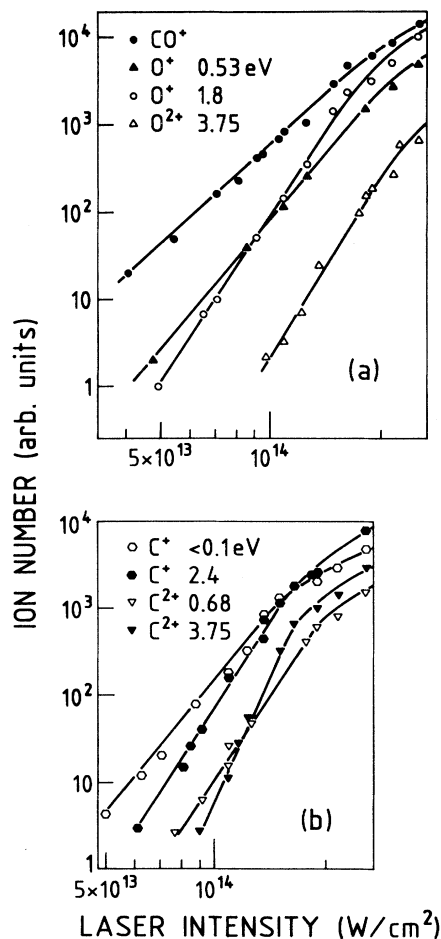
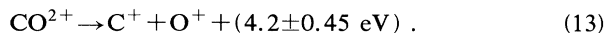


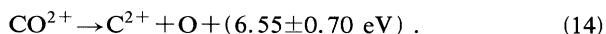
FIG. 10. Number of ions collected as a function of peak laser intensity at 305 nm: (a) O^{p+} fragments, (b) C^{q+} fragments. The different classes of ion fragments are identified by their respective energies indicated in eV.

fulfill perfectly relation (1). Moreover, they have the same abundances and vary identically as a function of the laser intensity (Fig. 10). Consequently, we assume that the 2.4-eV C^+ and 1.8-eV O^+ ions result from the fragmentation of the same CO^{2+} parent ion according to

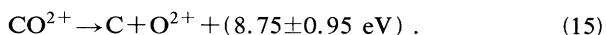


Comparison with *ab initio* calculations shows that several low-lying quasibound states of CO^{2+} can dissociate into fragments with such initial kinetic energies.¹⁵ For example, the production of a $C^+(^2P_u) + O^+(^4S_u)$ pair from the population of the $1^3\Pi$ state or the dissociation of CO^{2+} into $C^+(^2P_u) + O^+(^2D_u)$ from $^3\Sigma^+$ are two mechanisms compatible with our results.

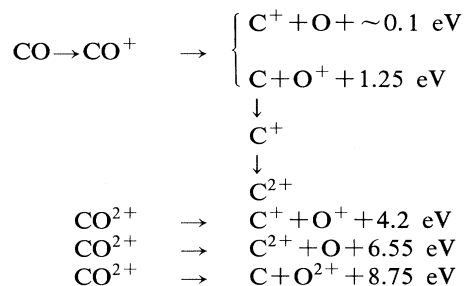
We note that two classes of doubly charged carbon fragments have appeared at 10^{14} W/cm². The faster C^{2+} ions are created with an energy of 3.75 eV and cannot be correlated with any O^+ ions (whose energies would be 2.8 eV). Thus we suppose that they are generated by the charge asymmetric reaction:



We observe that for each class of ions, the fast species become predominant at 3×10^{14} W/cm² [Fig. 8(c)]. Moreover, a small contribution of O^{2+} ions is detected at this laser intensity. They are interpreted as arising from a dissociative mechanism involving a high excited state of CO^{2+} :



In conclusion, we suggest the following sequence of events at 350 nm:



It is important to note that we do not observe the MPI of the neutral fragments arising from the dissociation of CO^{2+} . Consequently, the lifetime (in presence of the laser pulse) of the CO^{2+} populated states is longer than the pulse duration which impedes stepwise ionization processes at increasing r values as observed at 610 nm. As observed previously on N_2 at 305 nm,⁵ the multiphoton transitions inducing the various ionization channels occur at about the equilibrium internuclear distance of CO.

V. CONCLUSION

The interaction of the CO molecule with intense laser radiation induces a multiple ionization of the molecule which subsequently dissociates into energetic fragments. The laser-intensity dependence of the interaction products and the kinetic-energy distribution of the atomic fragments allow one to determine several aspects of the interaction process.

At 610 nm, the results show that the double ionization of CO is followed by the dissociation of the molecule before the extinction of the laser pulse. At sufficiently high laser intensity, a third electron is stripped away from the molecular ion during the dissociation process. The triple ionization occurs at two fixed internuclear distances corresponding to the creation of two dissociative states of CO^{3+} . The last step compatible with our laser intensity is the production of transient CO^{4+} ions at $r=3.6$ Å which dissociate into charge asymmetric C^{3+} and O^+ ions. These results confirm the nonvertical multiple ionization processes observed on N_2 at 600 (Ref. 4) and 610 nm.⁵ However, differences appear between the N_2 and CO results since higher charge states have been reached in N_2 and the charge symmetric dissociative channels are more favored in N_2 . In both cases, the successive ionization steps (up to the fourth molecular ionization) happen around the internuclear distance of about 3 Å where molecular binding and nonbinding forces are presumably still effective. In this case, (quasi) resonances between molecular states and the laser radiation could occur at given internuclear distances favoring the ionization processes at these distances.

At 305 nm, the experimental results indicate that the multiple ionization of CO progresses in a vertical way. This can be related to the nature of the CO^{2+} populated states which do not dissociate during the application of the laser pulse. Consequently, the multiphoton excitation of the molecule occurs at the internuclear separation of CO^{2+} quasibound states and results in the population of highly excited states correlating to the $C^{2+} + O$ and $C + O^{2+}$ separated atom limits. Such ionization mechanisms have been observed in N_2 at 248 (Refs. 3 and 8) and 305 nm.⁵

As a final remark, it is clear from our results that different levels of CO^{2+} are populated at 305 and 610 nm [reactions (5) and (13)] highlighting the role of the molecular structure even in the 10^{14} – 10^{15} W/cm² laser-intensity range. The experimental findings to be explained in future works concern (i) The nature of the molecular states populated—at each wavelength—during the successive ionization steps; (ii) the selectivity of the laser excitation (very few double charged molecular states are populated), and (iii) the possible occurrence of laser-induced (quasi) resonances to explain the ionization steps at well-defined internuclear separations.

¹K. Codling, L. J. Frasinski, and P. A. Hatherly, *J. Phys. B* **21**, L433 (1988).

²T. S. Luk and C. K. Rhodes, *Phys. Rev. A* **38**, 6180 (1988).

³K. Boyer, T. S. Luk, J. C. Solem, and C. K. Rhodes, *Phys. Rev.*

A **39**, 1186 (1989).

⁴L. J. Frasinski, K. Codling, and P. A. Hatherly, *Phys. Lett. A* **142**, 499 (1989).

⁵C. Cornaggia, J. Lavancier, D. Normand, J. Morellec, and H.

- X. Liu, *Phys. Rev. A* **42**, 5464 (1990).
- ⁶K. Codling, L. J. Frasinski, P. A. Hatherly, and M. Stankiewicz, *Phys. Scr.* **41**, 433 (1990).
- ⁷K. Codling, L. J. Frasinski, P. Hatherly, and J. Barr, *J. Phys. B* **20**, L525 (1987).
- ⁸G. Gibson, T. S. Luk, A. McPherson, K. Boyer, and C. K. Rhodes, *Phys. Rev. A* **40**, 2378 (1989).
- ⁹K. Codling, L. J. Frasinski, and P. A. Hatherly, *J. Phys. B* **22**, L321 (1989).
- ¹⁰L. A. Lompré, G. Mainfray, and J. Thebault, *Rev. Phys. Appl.* **17**, 21 (1982).
- ¹¹W. C. Wiley, and I. H. McLaren, *Rev. Sci. Instrum.* **26**, 1150 (1955).
- ¹²D. Normand, C. Cornaggia, J. Lavancier, J. Morellec, and H. X. Liu (unpublished).
- ¹³R. W. Wetmore, R. J. Le Roy, and R. K. Boyd, *J. Phys. Chem.* **88**, 6318 (1984).
- ¹⁴M. Larsson, B. J. Olsson, and P. Gigray, *Chem. Phys.* **139**, 457 (1989).
- ¹⁵P. Lablanquie, J. Delwiche, M.-J. Hubin-Franskin, I. Nenner, P. Morin, K. Ito, J. H. D. Eland, J.-M. Robbe, G. Gandara, J. Fournier, and P. G. Fournier, *Phys. Rev. A* **40**, 5673 (1989).
- ¹⁶A. S. Newton and A. F. Sciamanna, *J. Chem. Phys.* **53**, 132 (1970).
- ¹⁷J. H. Beynon, R. M. Caprioli, and J. W. Richardson, *J. Am. Chem. Soc.* **93**, 1852 (1971).
- ¹⁸J. M. Curtis and R. K. Boyd, *J. Chem. Phys.* **80**, 1150 (1984).
- ¹⁹G. Dujardin, L. Hellner, M. Hamdan, A. G. Brenton, B. J. Olsson, and Besnard-Ramage, *J. Phys. B* **23**, 1165 (1990).
- ²⁰B. Schram, A. Boerboom, W. Kleine, and J. Kistemaker (unpublished).
- ²¹R. R. Freeman, P. H. Bucksbaum, H. Milchberg, S. Darack, D. Schumacher, and G. M. Geusic, *Phys. Rev. Lett.* **59**, 847 (1987).
- ²²P. Agostini, P. Breger, A. L'Huillier, H. G. Muller, G. Petite, A. Antonetti, and A. Migus, *Phys. Rev. Lett.* **63**, 2208 (1989).